Effects of Different Electrolytes on Microstructure and Antibacterial Properties of Microarc Oxidized Coatings of CP-Ti

L. C. Tsao

***Abstract*—Titania-based coatings on commercially pure titanium (CP-Ti) were formed by micro-arc oxidation in different electrolyte solutions containing anions such as phosphate (PO_4^{3-}) and silicate (SiO_3^{2-}). The surface topography, phases, and elemental compositions of the P-TiO_2 and Si-TiO_2 coatings were characterized by scanning electron microscopy (SEM), energy-dispersive X-ray spectrometry (EDS), and X-ray diffraction (XRD), respectively. *Staphylococcus aureus (S. aureus)* was used to evaluate the antibacterial properties of the MAO coatings. The experimental results demonstrate that The P-TiO_2 coated sample had amorphous phase, main anatase-TiO_2, and a small amount of P_2O_5. However, the Si-TiO_2 coated samples were composed of SiO_2, anatase-TiO_2, and amorphous phase. After 24 h of incubation, the antibacterial activities against *S. aureus* were 96.4% for the P-TiO_2 coated sample and 98.6 % for the Si-TiO_2 coated sample.**

***Index Terms*—Commercially pure titanium, micro arc oxidation, corrosion, antibacterial property.**

I. Introduction

Ti and Ti-based alloys are extensively used in many applications, from aerospace to the biomedical sciences. They have excellent properties, such as high specific strength, good formability, corrosion resistance**,** non-toxicity, and excellent biocompatibility [1], [2]. New titanium alloys for biomaterials such as Ti-Nb [3], Ti-Cu [4], Ti-Cu-Sn [5] have been developed.

The good biocompatibility and corrosion resistance of these materials are attributed to a thin oxide layer (TiO_2 in case of titanium) that forms naturally on the surface of titanium. Typically, the thin oxide layers that form on these metals have an amorphous structure, film thickness of about 3-10 nm, and stoichiometric problems [6]. It is known that the stability of the oxide depends strongly on the composition structure and thickness of the film [7]. Therefore, they are usually used with protective coatings [8].

Various surface modification technologies have been studied for use with Ti and its alloys, examples being anodizing [9], physical vapor deposition (PVD) [10], plasma and laser nitriding [11], and ion implantation surface treatment [12]. In recent years, micro-arc oxidation (MAO) has proven to be a promising surface coating technology for forming thick oxide coatings on aluminum (Al), titanium (Ti), and magnesium (Mg) components [13], [14] and [15]. These thick oxide coatings have a hard ceramic property, good wear resistance, high corrosion resistance, and especially good adhesion between metal and coating in comparison with the conventional anodizing. Chang *et al.* [16] reported that microstructure characterization of the oxidized TiO_2 layer can be greatly affected by the discharge voltage on CP-Ti alloy during MAO treatment. Generally, current density is one of the most important parameters affecting the microstructure and properties of the MAO coating. However, little research has focused on the effects of different electrolytes on oxide coatings on CP-Ti alloys.

In the present study, the effects of different electrolyte systems on the formation of micro arc oxidation ceramic coatings of CP-Ti alloy were analyzed. The morphology, microstructure, phase constituents, corrosion resistance, and antibacterial activity of the MAO coatings were analyzed. The corrosion behavior was also evaluated by potentiodynamic polarization in 3.5 wt.% NaCl solution.

II. Materials and Methods

A. Preparation of Samples

The nominal composition of commercially pure titanium (CP-Ti) is shown in Table I. The specimens were cut into squares 20.0 × 20.0 × 1.0 mm, which were polished with different grades of emery papers up to 800 grits and then degreased in pure ethanol alcohol under ultrasonic conditions. The micro-arc oxidization treatment device, illustrated in Fig. 1a [17], consisted of a DC power supply unit, a 316 stainless steel container that also served as the counter electrode and a stirring and cooling system; the samples served as the anode.

TABLE I: Chemical Composition of CP-Ti (wt.%).

Fe	N	H	O	Si	Ti
0.08	0.02	0.012	0.10	<0.04	Bal.

The constant current density, applied DC voltage, and duration time were fixed at 33A/dm^2, 350V and 30 min, respectively. The electrolyte temperature was maintained within 20 ±2 ℃. To investigate the influence of electrolyte in the MAO process, the experiment was performed in two

Manuscript received October 24, 2019; revised February 8, 2020. This work was supported in part by the Ministry of Science and Technology, Taiwan, under Project No. MOST 107–222–E–020–011–MY2.

L. C. Tsao is with the Department of Materials Science and Engineering, National Pingtung University of Science and Technology, Pingtung, 91201Taiwan (e-mail: tlclung@mail.npust.edu.tw).

different solutions. For P-TiO_2 coating samples, the CP-Ti plates were treated by MAO in 10g/L H_3PO_4 solution. The Si-TiO_2 coating samples were treated by MAO in 10 g/L NaH_2PO_3 and 20 g/L Na_2SiO_3 solution. After the MAO processes, samples were cleaned with distilled water and then dried in hot air.

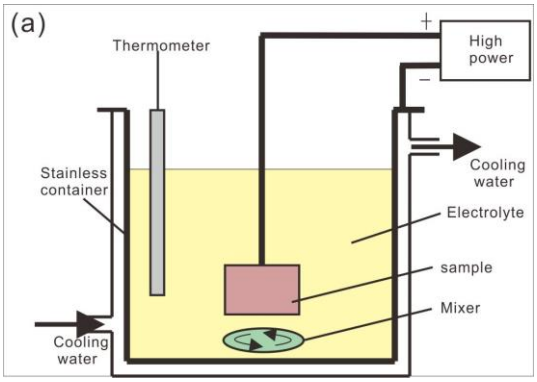

Fig. 1. Device for MAO treatment [17].

B. Microstructure Analysis

The surface morphology and composition of the treated samples were observed by scanning electron microscopy (SEM) (SEM, Hitachi S-4700, Japan) and energy-dispersive X-ray spectroscopy (EDS, XFlash detector 4010, Bruker, Germany). The crystal phase of the MAO coating sample was analyzed by X-ray diffractometry (XRD, Dmax III-A type, Rigaku Co., Japan) using Cu Kα radiation (λ= 1.5406 Å), a tube voltage of 40 kV, a current of 40 mA, and the 2θ range of 20-80 º.

C. Corrosion Behavior

Corrosion behavior of the coatings in electrochemical polarization experiments was initiated using a typical three-electrode cell, no stirring, and degassing of the solution at room temperature by an EG & G M273A potentiostat. The reference potential was a saturated calomel electrode (SCE) and a platinum (Pt) counter electrode (diameter 1.5 mm, 20 cm length). All electrolytes were prepared by dissolving high-grade chemicals in high purity deionized water (Millipore Milli-Q SP, 18 MΩ-cm). The specimen surfaces, with an area of approximately 2.829 cm^2, were exposed to the 3.5 wt.% NaCl solution at 25 ℃. For dynamic polarization testing, the potential began at –1.0 V_{SCE} and scanned in the noble direction to an anodic 2 V_{SCE} at a scanning rate of 1 mV/s.

D. Antibacterial Activity Tests

The photocatalytic activities of P-TiO_2 and Si-TiO_2 matrices were evaluated against *S. aureus* under visible light at room temperature (25 ± 2 ℃) by % viability (% survival) of bacteria. The MAO coating samples were sterilized by autoclave at 120 ℃ for 30 min. The antimicrobial effect was evaluated with the Japanese Industrial Standard (JIS) Z2801:2000 method. This standard is commonly used to estimate the antimicrobial abilities of antimicrobial products [18], [19]. The MAO sample sizes were 5.0 × 5.0 cm. After culture medium containing bacteria (about 0.4 ml) was dripped onto the MAO samples, the samples were covered with film (4.0 × 4.0 cm).

The cell culture medium was a nutrient broth with distilled water diluted 500-fold. The nutrient broth was prepared by diluting beef extract (3.0 g), peptone (10.0 g), and sodium chloride (5.0 g) in purified water (1000 g), with the pH adjusted to7.0 ±0.2 using sodium hydroxide or hydrochloric acid.

The bacterial solution with a concentration of 1.8×10^5 CFUs/mL was dripped onto the surface of MAO samples at a density of 0.05 mL/cm^2. After the bacteria were cultured for 24 h at 35±1 ℃, the bacteria CFUs were counted in the whole culture. The antibacterial activity was calculated using the following formula [20]:

$$R = (N_{control} - N_{sample})/N_{control} \times 100\% \quad (1)$$

where $N_{control}$ is the average number of the bacterial colony on the control sample at 24 h, and N_{sample} is the average number of the bacterial colony on the MAO sample at 24 h.

TABLE II: EDS ANALYSIS RESULTS OF INDICATED ZONE IN FIG. 2.

Samples	Composition (wt.%)				Phase identification
	Ti	O	P	Si	
P-TiO_2	18.96	75.27	5.78	-	$TiO_2 + P_2O_7$
Si-TiO_2	8.76	76.69	1.41	13.13	$TiO_2 + SiO_2$

III. RESULTS AND DISCUSSION

A. Microstructures

Fig. 2 shows the surface morphologies of the coatings prepared in different electrolytes. It can be clearly observed that the coatings exhibited quite different surface morphologies in the different electrolytes. The surfaces of the P-TiO_2 coating samples displayed rough topographies, and the surfaces contained numerous micropores or crater structures, separately and homogeneously distributed over the coatings (Fig. 2a). In our previous study [21], the same phenomenon was also observed. However, the surfaces of the Si-TiO_2 coating samples displayed smooth topographies and few micropores. The density of the micropores on the P-TiO_2 coating sample was higher than that on the Si-TiO_2 coating sample. The cross section and thickness of the coatings prepared in different electrolytes are shown in Figs. 3 and 4, respectively. The thicknesses were approximately 3.25 ± 0.48μm for the P-TiO_2 coating sample and 11.35 ± 0.61μm for the Si-TiO_2 coating sample, respectively. Jiang *et al.* reported that the adsorption degree of ceramic coatings is in the order of $SiO_3^{2-} > PO_4^{3-} > VO_4^{3-} > MoO_4^{2-} > B_4O_7^{2-} > CrO_4^{2-}$ [22].

Fig. 5 summarizes the elemental compositions of the P-TiO_2 coating and Si-TiO_2 coating samples determined on their surfaces by energy dispersive spectroscopy (EDS). The results are summarized in Table 2. Only Ti (18.96 wt.%), O (75.27 wt.%) and P (5.78 wt.%) were detected in the P-TiO_2 coating samples. These results suggest that the coating film contained TiO_2 and P_2O_7 phase [21]. In previous work, the TiO_2 films were formed on CP-Ti by MAO process by the following steps [23], [24]:

$$Ti/Ti: Ti \leftrightarrow Ti^{2+} + 2e^{-} \quad (1)$$

$$2H_2O \leftrightarrow 2O^{2-} + 4H^{+} \quad (2)$$

$$2H_2O \rightarrow O_2\,(gas) + 4H^{+} + 4e^{-} \quad (3)$$

$$Ti^{2+} + 2O^{2-} \rightarrow TiO_2 + 2e^{-} \quad (4)$$

Thus, TiO_2 is major phase in the MAO coating process. Furthermore, it has been reported that both P_2O_5 and titanium pyrophosphate (TiP_2O_7) have been deposited on a sample surface [21]. In Si-TiO_2 coating samples, the elemental composition was Ti (8.76 wt.%), O (75.27wt.%), Si (13.13 wt.%) and traces of P (1.41 wt.%). This composition suggests that the Si-TiO_2 coating samples had TiO_2 and SiO_2 phases.

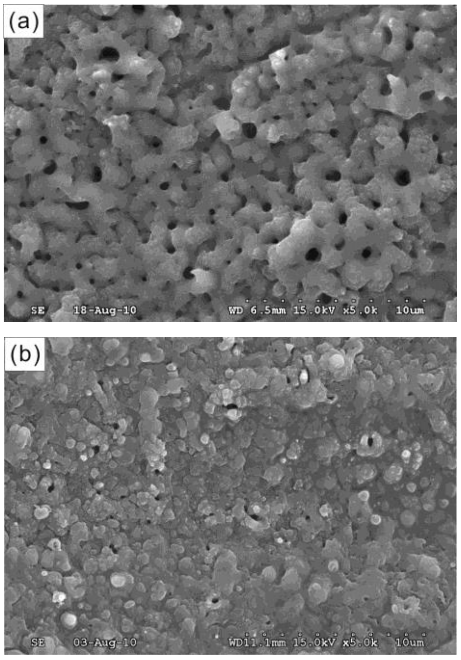

Fig. 2. Morphologies of the MAO coating formed on CP-Ti: (a) P-TiO_2 sample; (b) Si –TiO_2 sample.

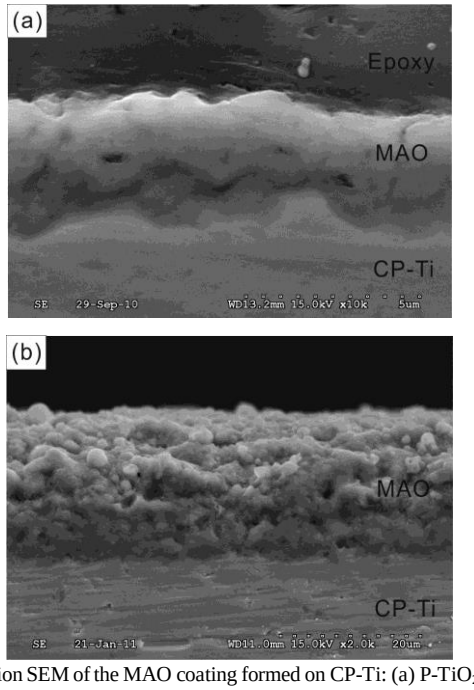

Fig. 3. Section SEM of the MAO coating formed on CP-Ti: (a) P-TiO_2 sample; (b) Si –TiO_2 sample.

Fig. 6 shows the XRD patterns of the MAO coating in different electrolytes. In the P-TiO_2 samples, the coating was composed of α-Ti, anatase TiO_2, amorphous phase, and a trace of P_2O_5, respectively. However, no rutile TiO_2 and TiP_2O_7 phases were observed. It is likely that the temperature of the sparking location did not reach the phase transfer temperature [25]. Also, it is obvious that the Si-TiO_2 coating samples consisted of α-Ti, anatase TiO_2, amorphous phase, and a trace of SiO_2.

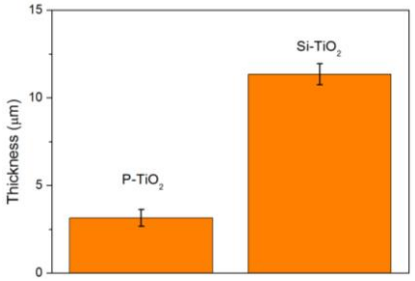

Fig. 4. Thickness of the formed MAO layer in different electrolytes.

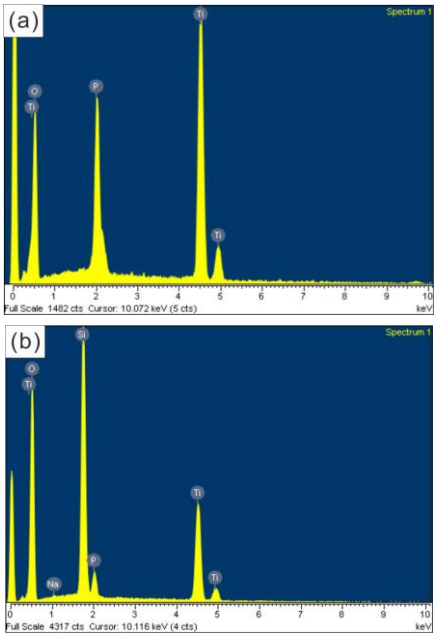

Fig. 5. EDS analysis of the MAO coating surface, (a) P-TiO_2 coating samples and (b) Si-TiO_2 coating samples.

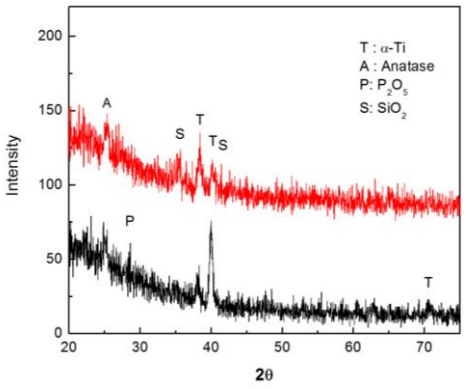

Fig. 6. XRD patterns of (a) P-TiO_2 coating samples and (b) Si-TiO_2 coating samples.

B. *Corrosion Behavior*

The potentiodynamic polarization curves of CP-Ti coated samples are shown in Fig. 7. The corrosion current density

(I_{corr}), corrosion potential (E_{corr}), critical current density (I_{crit}) and polarization resistance (R_p), obtained by fitting the polarization curves, are listed in Table III. Polarization resistance (R_p) has been used for the kinetics of electrode reactions that can be calculated from the equilibrium potential [26]. It corresponds to the endurable degree of corrosion process [27]. R_p is defined as [28]:

$$R_p = \left|\frac{dE}{dI}\right|_{E-E_{corr}\sim 0} \quad (5)$$

According to the Stern–Geary equation [29], the analysis of the R_p of MAO coating samples was based on the E_{corr}, I_{corr} and the anodic/cathodic Tafel slopes (β_a and β_c), which were obtained from the measured polarization curves. The corrosion resistance (R_p) value was determined from the relationship [26], [29]:

$$R_p = \left(\frac{1}{2.303 I_{corr}}\right)\left(\frac{\beta_a \beta_c}{\beta_a + \beta_c}\right) \quad (6)$$

For P-TiO_2 coating samples, E_{corr} = -170.8 mV_{SCE}, I_{corr} = 1.75 μA/cm^2, I_{crit} = 6.09 μA/cm^2 were measured. However, the Si-TiO_2 coating samples exhibited an obvious shift in E_{corr} toward the noble direction (-140.7 mV_{SCE}), and a significant one-order decrease in both I_{corr} (0.37μA/cm^2) and I_{crit} (6.09μA/cm^2). These data corroborated their R_p values. The corrosion resistance of Si-TiO_2 coating samples was higher than that of P-TiO_2 coating samples. The MAO coating developed in the electrolyte solution containing $NaSiO_3$ had the highest corrosion resistance of SiO_2 phase as compared to the P_2O_5 phase in the P-TiO_2 coating samples. In addition, the corrosion behavior of MAO coated samples had better corrosion resistance than CP-Ti alloy untreated substrate (Table III). Hence, it is clear that the corrosion resistance of CP-Ti was significantly enhanced by the MAO coating process.

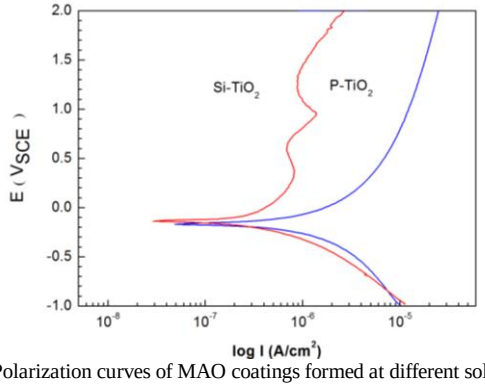

Fig. 7. Polarization curves of MAO coatings formed at different solution.

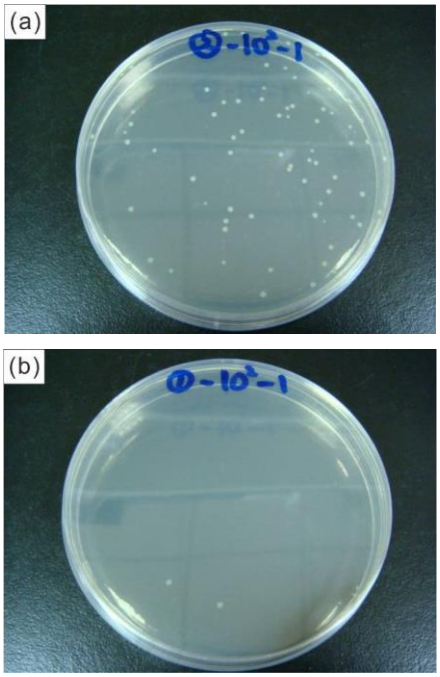

Fig. 8. *S. aureus* bacterial colonies after incubation for 24 h on different samples. (a) P-TiO_2 coating samples and (b) Si-TiO_2 coating samples.

TABLE III: THE RESULTS OF POTENTIODYNAMIC CORROSION TESTS IN A 3.5 WT. % NACL SOLUTIONS

Samples	E_{corr}(mV_{SCE})	I_{corr} (μA/cm^2)	I_{crit} (μA/cm^2)	β_a (mV/decade)	β_c (mV/decade)	R_p (Ohms/cm^2)
P-TiO_2	-170.8	1.75	6.09	1019.2	-833.1	1132.1
Si-TiO_2	-140.7	0.37	0.48	1031.1	-718	2774.9

TABLE IV: COLONY NUMBERS AND THE ANTIBACTERIAL ACTIVITY FOR DIFFERENT SAMPLES AGAINST *S. AUREUS* BACTERIA.

Sample	Negative sample(CFU/ml)	No. of bacteria on the coated samples after 24 h (CFU/ml)	Antibacterial activity(%)
P-TiO_2	1.8×10	6.4×10	96.4
Si-TiO_2	1.8×10	2.5×10	98.6

C. Antibacterial Property

Before the antibacterial behavior of MAO coating samples was examined, a bacterial growth curve for *S. aureus* was developed. Fig. 8 shows the photos of colony forming units of viable *S. aureus* after contact with the MOA samples. When exposed to *S. aureus*, MAO coating samples showed good antibacterial properties, with a kill rate of 96.4 %. Compared to the P-TiO_2 coating samples (96.4 %), Si-TiO_2 coating samples (98.6 %) exhibited a stronger antibacterial action due to the higher concentration of Si in the MAO coated surfaces (Table IV). There are many factors that may reduce bacterial counts on MAO coated samples, such as the morphology, the surface free energy, and the material modified (Ag, Cu, SiO_2). The coating surface is critical to its antibacterial effects. Both Ag and Cu are widely known to be antibacterial agents [30], [31]. Zhang *et al.* reported that a Ag-modified TiO_2 coating showed excellent antibacterial activity against *Escherichia coli* (*E. coli*) within 24 h and that the antibacterial rate gradually rose with increasing contact time [30]. Zhu *et al.* reported that Cu-incorporated TiO_2 coatings were highly effective at inhibiting the adhesion of *S. aureus* and exhibited excellent biological activity in promoting osteoblastic adhesion, early

proliferation, and late differentiation [31]. Furthermore, silica nanoparticles have high thermal and chemical stability, high surface area, and good biocompatibility, making them a good option for delivering drugs such as antibiotics [32], [33] and [34]. It is demonstrated that MAO layers incorporating Si can enhance antimicrobial properties.

IV. Conclusions

In summary, the MAO technique has successfully been used in this study to grow TiO_2 on CP-Ti alloy in different electrolytes. After the MAO process, the P-TiO_2 sample surface was rough and porous, with largely micro-sized pores. The P-TiO_2 film had amorphous phase, main anatase-TiO_2, and a small amount of P_2O_5. However, the Si-TiO_2 sample surface was smooth and had few nano-sized pores. The Si-TiO_2 films were composed of SiO_2, anatase-TiO_2, and amorphous phase. It was found that the MAO coatings significantly improved the corrosion behavior of the CP-Ti substrate. The corrosion protection of the Si-TiO_2 coated sample was better than that of the P-TiO_2 coated sample. The antibacterial activities against *S. aureus* at 24 h were 96.4% for the P-TiO_2 coated sample and 98.6 % for the Si-TiO_2 coated sample.

Acknowledgment

The authors acknowledge the financial support of this work from the Ministry of Science and Technology, Taiwan, under Project No. MOST 107-222-E-020-011-MY2. SEM was performed by the Precision Instrument Center of National Pingtung University of Science and Technology, Taiwan.

Conflict of Interest

The authors declare no conflict of interest.

Author Contributions

Tsao author carry out all works.

References

[1] L. C. Tsao, H. Y. Wu, J. C. Leong, and C. J. Fang, "Flow stress behavior of commercial pure titanium sheet during warm tensile deformation," *Mater. Design*, vol. 34, pp. 179-184, 2012.

[2] S. Nag and R. Banerjee, "Fundamentals of medical implant materials," *ASM Handbook*, Materials for Medical Devices (R. Narayan, Ed.), vol. 23, pp. 6-17, 2012.

[3] A. Cremasco, W. R. Os ório, C. M. A. Freire, A. Garcia, and R. Caram, "Electrochemical corrosion behavior of a Ti–35Nb alloy for medical prostheses," *Electrochimica Acta*, vol. 53, pp. 4867-4874, 2008.

[4] L. C. Tsao, "Basic electrochemical behavior of Ti-7Cu alloys for medical applications," *Acta Phys. Pol. A*, vol. 122, 561-564, 2012.

[5] L. C. Tsao, Formation of ultrafine structure in as cast Ti7CuXSn alloys," *Mater. Sci.Tech*., vol. 29, pp. 1529 -1536, 2013.

[6] K. G. Neoh, X. Hu, D. Zheng, and E. T. Kang, "Balancing osteoblast functions and bacterial adhesion on functionalized titanium surfaces," *Biomater*., vol. 33, pp. 2813-2822, 2012.

[7] X. Zhu, J. Chen, L. Scheideler, R. R. Reichl, and J. Geis-Gerstorfer, "Effects of topography and composition of titanium surface oxides on osteoblast responses," *Biomater*., vol. 25, pp.4087-4103, 2004.

[8] T. Moskalewicz, F. Smeacetto, and A. Czyrska-Filemonowicz, "Microstructure, properties and oxidation behavior of the glass-ceramic based coating on near-α titanium alloy," *Surf. Coat. Technol.*, vol. 203, pp. 2249-2253, 2009.

[9] L. P. He, Y. W. Mai, and Z. Z. Chen, "Fabrication and characterization of nanometer CaP(aggregate)/Al_2O_3 composite coating on titanium," *Mater. Sci. Eng. A*, vol. 367, pp. 51-56, 2004.

[10] M. S. F. Lima, F. Folio, and S. Mischler, "Microstructure and surface properties of laser-remelted titanium nitride coatings on titanium," *Surf. Coat. Technol*., vol. 199, pp.83-91, 2005.

[11] H. C. Man, Z. D. Cui, T. M. Yue, and F. T. Cheng, "Cavitation erosion behavior of laser gas nitrided Ti and Ti6Al4V Alloy," *Mater. Sci. Eng. A*, vol. 355, pp. 167-173, 2003.

[12] K. Asami, N. Ohtsu, K. Saito, and T. Hanawa, "$CaTiO_3$ films sputter-deposited under simultaneous Ti-ion implantation on Ti-substrate," *Electrochim. Acta*, vol. 200, pp. 1005–1008, 2005.

[13] Z. Huan, L. E. Fratila-Apachitei, I. Apachitei, and J. Duszczyk, "Porous NiTi surfaces for biomedical applications," *Appl. Surf. Sci.*, vol. 258, pp. 5244-5249, 2012.

[14] G. H. Lv, H. Chen, W. C. Gu, L. Li, E. W. Niu, X. H. Zhang, and S. Z. Yang, "Effects of current frequency on the structural characteristics and corrosion property of ceramic coatings formed on magnesium alloy by PEO technology," *J. Mater. Process. Technol*., vol. 208, pp. 9-13, 2008.

[15] T.H. Teh, A. Berkani, S. Mato, P. Skeldon, G. E. Thompson, H. Habazaki, and K. Shimizu, "Initial stages of plasma electrolytic oxidation of titanium," *Corr. Sci.*, vol. 45, pp. 2757-2768, 2003.

[16] S. Y. Chang, H. K. Lin, L. C. Tsao, W. T. Huang, and Y. T. Huang, "Effect of voltage on microstructure and corrosion resistance of microarc oxidation coatings on CP-Ti," *Corr. Eng. Sci. Tech*., vol. 49, pp. 17-22, 2014.

[17] L. C. Tsao, "Interfacial structure and fracture behavior of 6061 Al and MAO-6061Al direct active soldered with Sn–Ag–Ti active solder," *Mater. Design*, vol. 56, pp. 318-324, 2014.

[18] Japanese Standards Association, "Antimicrobial products: Test for antimicrobial activity and efficacy," Japanese Industrial Standard 2000, JIS Z 2801.

[19] K. Tamai, K. Kawate, I. Kawahara, Y. Takakura, and K. Sakaki, "Inorganic antimicrobial coating for titanium alloy and its effect on bacteria," *J. Orthop. Sci.*, vol. 14, pp. 204-209.

[20] B. Erdural, U. Bolukbasi, and G. Karakas, "Photocatalytic antibacterial activity of TiO_2–SiO_2 thin films: The effect of composition on cell adhesion and antibacterial activity," *J. Photochem. Photobiol. Chem*., vol. 283, pp. 29-37.

[21] S. Y. Chang, H. K. Lin, L. C. Tsao, W. T. Huang, and Y. T. Huang, "Effect of voltage on microstructure and corrosion resistance of microarc oxidation coatings on CP-Ti," *Corros. Eng. Sci. Tech.*, vol. 49, pp. 17-22, 2014.

[22] Y. F. Jiang, J. M. Li, B. L. Jiang, and C. P. Fu, "Jiang analysis of formed factors of micro-arc oxidation ceramic coating, *Surf. Coat. Technol.* vol. 30, pp. 37-39, 2001.

[23] D. M. Brunette, P. Tengvall, M. Textor, and P. Thomsen, "Titanium in medicine," *Springer*, pp. 247-255, 2001.

[24] T. Y. Park, S. H. Eom, M. D. Kim, S. H. Kim, H. L. Kim, G. R. Jeon, H. J. Shin, and J. W. Shin, *OSSTEM Implant System*, pp. 506-517, 2005.

[25] J. Yahalom and J. Zahavi, "Electrolytic breakdown crystallization of anodic oxide films on breakdown hypotheses," *Electrochim. Acta*, vol. 16, pp. 603-607, 1971.

[26] J. L. Fernandez, M. R. G. de Chialvo, and A. C. Chialvo, "Kinetic study of the chlorine electrode reaction on Ti/RuO_2 through the polarisation resistance Part II: Mechanistic analysis," *Electrochim. Acta*, vol. 47, pp. 1137-1144, 2002.

[27] R. P. Khatri, V. Sirivivatnanon, and P. Heeley, "Critical polarization resistance in service life determination," *Cement Concr. Res.*, vol. 34, pp. 829-837, 2004.

[28] D. Chidambaram, C. R. Clayton, and M. R. Dorfman, "Evaluation of the electrochemical behavior of HVOF-sprayed alloy coatings," *Surf. Coat. Tech.*, vol. 176, pp. 307-317, 2004.

[29] M. Stern and A. L. Geary, "Electrochemical polarization. A theoretical analysis of shape of polarization curves," *J. Electrochem. Soc.*, vol. 104, pp. 56-63, 1957.

[30] X. G. Zhang, R. Q. Hang, H. Wu, X. B. Huang, Y. Ma, N. M. Lin, X. H. Yao, L. H. Tian, and B. Tang, "Synthesis and antibacterial property of Ag-containing TiO_2 coatings by combining magnetron sputtering with micro-arc oxidation, *Surf. Coat. Tech.*, vol. 235, pp.748-754, 2013.

[31] W. Zhu, Z. X. Zhang, B. B. Gu, J. Y. Sun, and L. X. Zhu, "Biological activity and antibacterial property of nano-structured TiO_2 coating incorporated with Cu prepared by micro-arc oxidation," *J. Mater. Sci. Technol.*, vol. 29, pp. 237-244, 2013.

[32] M. Foglia, G. Alvarez, P. Catalano, A. Mebert, L. Diaz, T. Coradin, and M. Desimone, "Recent patents on the synthesis and application of silica nanoparticles for drug delivery," *Recent Patents on Biotechnol.*, vol. 5, pp. 54-61, 2011.

[33] A. M. Mebert, D. E. Camporotondi, M. L. Foglia, G. S. Alvarez, P. L. S. Orihuela, L. E. Diaz, and M. F. Desimone, "Controlling the interaction

between cells and silica nanoparticles," *J. Biomater. Tissue Eng.*, vol. 3, pp.108-121, 2013

[34] D. E. Camporotondi, M. L. Foglia, G. S. Alvarez, A. M. Mebert, L. E. Diaza, T. Coradin, and M. F. Desimone, "Antimicrobial properties of silica modified nanoparticles, Microbial pathogens and strategies for combating them: Science, technology and education," pp. 283-290, 2013..

L. C. Tsao is a professor in the National Pingtung University of Science and Technology, College of Engineering, Graduate institute of Materials Engineering. He received his BS in industry education from Nation Taiwan normal University, MS in engineering from National Center University and PhD in Material Science from National Taiwan University.

His research interests cover art material, jewelry design, brazing and casting, with emphasis on materials characterization and the application of materials and mechanical engineering fundamentals to product design. His current research interests are in the areas of the light alloy, 3D powder, special filler, art material and jewelry design.